



International
Standard

ISO 25498

**Microbeam analysis — Analytical
electron microscopy — Selected
area electron diffraction analysis
using a transmission electron
microscope**

*Analyse par microfaisceaux — Microscopie électronique
analytique — Analyse par diffraction par sélection d'aire au
moyen d'un microscope électronique en transmission*

**Third edition
2025-05**



COPYRIGHT PROTECTED DOCUMENT

© ISO 2025

All rights reserved. Unless otherwise specified, or required in the context of its implementation, no part of this publication may be reproduced or utilized otherwise in any form or by any means, electronic or mechanical, including photocopying, or posting on the internet or an intranet, without prior written permission. Permission can be requested from either ISO at the address below or ISO's member body in the country of the requester.

ISO copyright office
CP 401 • Ch. de Blandonnet 8
CH-1214 Vernier, Geneva
Phone: +41 22 749 01 11
Email: copyright@iso.org
Website: www.iso.org

Published in Switzerland

Contents		Page
Foreword.....		iv
Introduction.....		v
1	Scope.....	1
2	Normative references.....	1
3	Terms, definitions and abbreviations.....	1
3.1	Terms and definitions.....	1
3.2	Abbreviated terms and symbols.....	3
4	Principle.....	3
4.1	General.....	3
4.2	Spot diffraction pattern.....	4
4.3	Kikuchi pattern.....	6
4.4	Diffraction pattern of polycrystalline specimen.....	7
5	Reference materials.....	8
6	Apparatus.....	8
6.1	Transmission electron microscope (TEM).....	8
6.2	Recording of SAED patterns and images.....	8
7	Preparation of specimens.....	9
8	Procedure.....	9
8.1	Instrument preparation.....	9
8.2	Procedure for acquiring SAED patterns from a single crystal.....	10
8.3	Determination of diffraction constant, $L\lambda$	12
9	Measurement and solution of the SAED patterns.....	14
9.1	Selection of the basic parallelogram.....	14
9.2	Indexing diffraction spots.....	15
10	180° ambiguity.....	16
11	Uncertainty estimation.....	16
11.1	General.....	16
11.2	Uncertainty in camera constant.....	17
11.3	Calibration with a reference material.....	17
11.4	Uncertainty in d -spacing values.....	18
Annex A (informative) Interplanar spacings of references.....		20
Annex B (informative) Spot diffraction patterns of single crystals for BCC, FCC and HCP structure [7].....		21
Bibliography.....		42

Foreword

ISO (the International Organization for Standardization) is a worldwide federation of national standards bodies (ISO member bodies). The work of preparing International Standards is normally carried out through ISO technical committees. Each member body interested in a subject for which a technical committee has been established has the right to be represented on that committee. International organizations, governmental and non-governmental, in liaison with ISO, also take part in the work. ISO collaborates closely with the International Electrotechnical Commission (IEC) on all matters of electrotechnical standardization.

The procedures used to develop this document and those intended for its further maintenance are described in the ISO/IEC Directives, Part 1. In particular, the different approval criteria needed for the different types of ISO document should be noted. This document was drafted in accordance with the editorial rules of the ISO/IEC Directives, Part 2 (see www.iso.org/directives).

ISO draws attention to the possibility that the implementation of this document may involve the use of (a) patent(s). ISO takes no position concerning the evidence, validity or applicability of any claimed patent rights in respect thereof. As of the date of publication of this document, ISO had not received notice of (a) patent(s) which may be required to implement this document. However, implementers are cautioned that this may not represent the latest information, which may be obtained from the patent database available at www.iso.org/patents. ISO shall not be held responsible for identifying any or all such patent rights.

Any trade name used in this document is information given for the convenience of users and does not constitute an endorsement.

For an explanation of the voluntary nature of standards, the meaning of ISO specific terms and expressions related to conformity assessment, as well as information about ISO's adherence to the World Trade Organization (WTO) principles in the Technical Barriers to Trade (TBT), see www.iso.org/iso/foreword.html.

This document was prepared by Technical Committee ISO/TC 202, *Microbeam analysis*, Subcommittee SC 3, *Analytical electron microscopy*.

This third edition cancels and replaces the second edition (ISO 25498:2018), which has been technically revised.

The main changes are as follows:

- Scope has been revised;
- ISO/IEC 17025 has been moved from normative references to bibliography;
- [Figure 1](#) has been replaced;
- Subclause 6.3 has been deleted;
- Subclause 8.3.6 has been deleted, the content of 8.3.6 has been moved to [8.3.2](#);
- [Subclause 9.2.5](#) has been added and the following subclause has been renumbered;
- [Clause 11](#) has been revised, [11.1](#), [11.2](#), [11.3](#) and [11.4](#) have been added;
- [Subclauses B.4.1](#) and [B.4.2](#) have been added;
- Bibliography has been updated and ISO/IEC Guide 98-3 (GUM:1995) has been added.

Any feedback or questions on this document should be directed to the user's national standards body. A complete listing of these bodies can be found at www.iso.org/members.html.

Introduction

Electron diffraction techniques are widely used in transmission electron microscopy (TEM) studies. Applications include phase identification, determination of the crystallographic lattice type and lattice parameters, crystal orientation and the orientation relationship between two phases, phase transformations, habit planes and defects, twins and interfaces, as well as studies of preferred crystal orientations (texture). While several complementary techniques have been developed, for example microdiffraction, nano-diffraction, convergent beam diffraction and reflected diffraction, the selected area electron diffraction (SAED) technique is the most frequently employed.

This technique allows direct analysis of small areas on thin specimens from a variety of crystalline substances. It is routinely performed on most TEMs in the world. The SAED is also a supplementary technique for acquisition of high-resolution images, microdiffraction or convergent beam diffraction studies. The information generated is widely applied in studies for the development of new materials, improving structure and/or properties of various materials as well as for inspection and quality control purpose.

The basic principle of the SAED method is described in this document. The experimental procedure for the acquirement of SAED patterns, indexing of the diffraction patterns and determination of the diffraction constant are specified. ISO 25498 is intended for use or reference as technical regulation for transmission electron microscopy.

Microbeam analysis — Analytical electron microscopy — Selected area electron diffraction analysis using a transmission electron microscope

1 Scope

This document specifies the method for selected area electron diffraction (SAED) analysis using a transmission electron microscope (TEM) to analyse thin crystalline specimens. This document applies to test areas of micrometres and sub-micrometres in size. The minimum diameter of the selected area in a specimen which can be analysed by this method is restricted by the spherical aberration coefficient of the objective lens of the microscope and approaches hundreds of nanometres for a modern TEM.

When the size of an analysed specimen area is smaller than the spherical aberration coefficient restriction, this document can also be used for the analysis procedure. However, because of the effect of spherical aberration and deviation of the specimen height position, some of the diffraction information in the pattern can be generated from outside of the area defined by the selected area aperture. In such cases, the use of microdiffraction (nano-beam diffraction) or convergent beam diffraction, where available, can be preferred.

This document is applicable to the acquisition of SAED patterns from crystalline specimens, indexing the patterns and calibration of the camera constant.

2 Normative references

There are no normative references in this document.

3 Terms, definitions and abbreviations

For the purposes of this document, the following terms and definitions apply.

ISO and IEC maintain terminology databases for use in standardization at the following addresses:

- ISO Online browsing platform: available at <https://www.iso.org/obp>
- IEC Electropedia: available at <https://www.electropedia.org/>

3.1 Terms and definitions

3.1.1

Miller notation

indexing system for crystallographic planes and directions in crystals, in which a set of lattice planes or directions is described by three axes coordinate

3.1.2

Miller-Bravais notation

indexing system for crystallographic planes and directions in hexagonal crystals, in which a set of lattice planes or directions is described by four axes coordinate

3.1.3

interplanar spacing

d_{hkl}

perpendicular distance between consecutive planes of the crystallographic plane set (hkl)

3.1.4 reciprocal vector

\mathbf{g}_{hkl}

vector in the reciprocal lattice

Note 1 to entry: The reciprocal vector, \mathbf{g}_{hkl} , is normal to the crystallographic plane $(h\ k\ l)$ with its magnitude inversely proportional to *interplanar spacing* d_{hkl} ([3.1.3](#)).

3.1.5 \mathbf{R} vector

\mathbf{R}_{hkl}

coordinate vector from the direct beam, 000, to a diffraction spot, hkl , in a zone diffraction pattern

Note 1 to entry: See [Figure 1](#).

3.1.6 camera length

L

effective distance from the specimen to the screen or recording device in a transmission electron microscope in diffraction mode

3.1.7 camera constant

diffraction constant

$L\lambda$

product of the wavelength of the incident electron wave and *camera length* ([3.1.6](#))

[SOURCE: ISO 15932:2013, 3.7.1]

3.1.8 bright field image

image formed using only the non-scattered beam, selected by observation of the back focal plane of the objective lens and using the objective aperture to cut out all diffracted beams

[SOURCE: ISO 15932:2013, 5.5]

3.1.9 dark field image

image formed by a diffracted beam only by using the objective aperture for selection or by collecting the diffracted beams with an annular dark-field detector

[SOURCE: ISO 15932:2013, 5.6]

3.1.10 energy-dispersive X-ray spectrometry

EDS

analytical technique which enables the elemental analysis or chemical characterization of a specimen by analysing characteristic X-ray emitted by the matter in response to electron irradiation

[SOURCE: ISO 15932:2013, 6.6]

3.1.11 eucentric position

specimen position at which the image exhibits minimal lateral motion resulting from specimen tilting

3.1.12 selected area (selector) aperture

moveable diaphragm that is used to select only radiation scattered from a specific area of the specimen to contribute to the formation of a diffraction pattern

[SOURCE: ISO 15932:2013, 3.2.3.5]

3.1.13
Bragg angle
 θ_B

angle between the incident beam and the atomic planes, at which diffraction takes place

3.2 Abbreviated terms and symbols

BCC	body-centred cubic structure
FCC	face-centred cubic structure
HCP	hexagonal close-packed structure
SAED	selected area electron diffraction
TEM	transmission electron microscope
(hkl)	<i>Miller indices</i> of a specific set of crystallographic planes
$\{hkl\}$	<i>Miller indices</i> which denote a family of crystallographic planes
$[uvw]$	<i>Miller indices</i> of a specific crystallographic direction or a zone axis
$(uvw)^*$	Notation for a set of planes in the reciprocal lattice

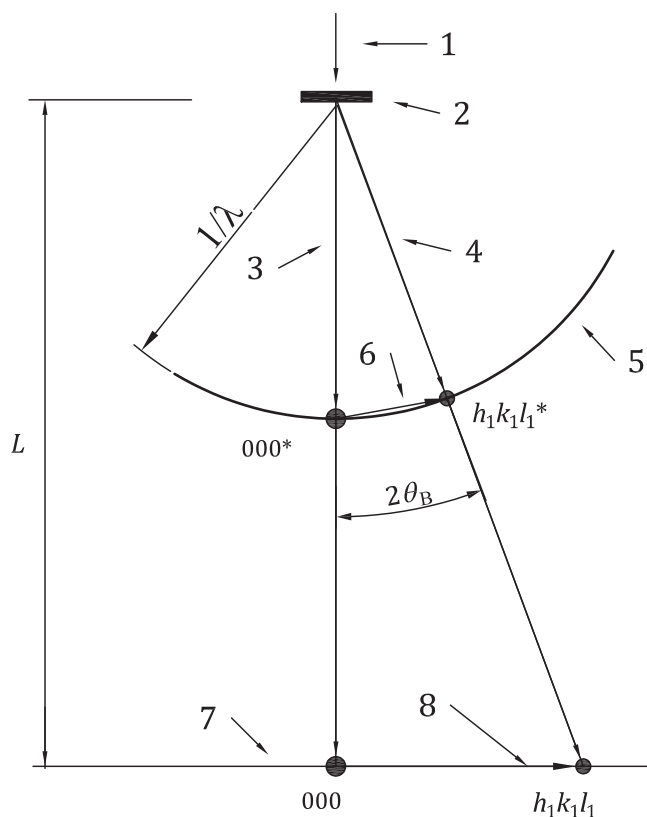
NOTE The normal of the reciprocal plane $(uvw)^*$ is parallel to the crystallographic zone axis $[uvw]$

4 Principle

4.1 General

When an energetic electron beam is incident upon a thin crystal specimen in a transmission electron microscope, a diffraction pattern will be produced in the back focal plane of the objective lens. This pattern is magnified by the intermediate and projector lenses, then displayed on a viewing screen and recorded (see Reference [3], [4], [5]). This pattern can also be displayed on a monitor if the TEM is equipped with a digital camera system.

The geometric relationship of the parameters for selected area electron diffraction (SAED) technique can be understood through the Ewald sphere construction, which is illustrated in [Figure 1](#).



Key

- 1 incident beam
- 2 specimen
- 3 direct beam
- 4 diffracted beam
- 5 Ewald sphere
- 6 reciprocal vector \mathbf{g}_{hkl}
- 7 diffraction pattern
- 8 \mathbf{R}_{hkl} vector
- L is the diffraction camera length;
- θ_B is Bragg angle;
- λ is the wavelength of the incident electron beam.

Figure 1 — Ewald sphere construction illustrating the diffraction geometry in TEM

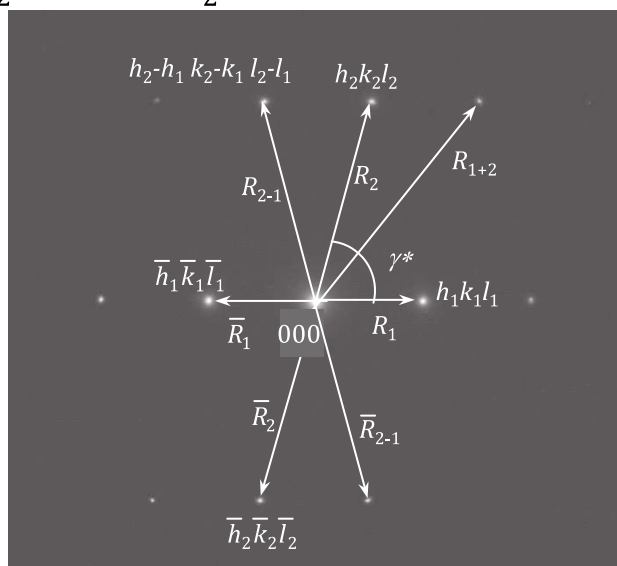
4.2 Spot diffraction pattern

The diffraction pattern of a single crystal appears as an array of “spots”, the basic unit of which is characterized by a parallelogram. An example of the spot diffraction pattern is shown in [Figure 2](#). Each spot corresponds to diffraction from a specific set of crystal lattice planes in the specimen, denoted by Miller indices (hkl) . The vector, \mathbf{R}_{hkl} , is defined by the position of the diffracted spot, hkl , relative to position on the pattern corresponding to the direct beam, i.e. the centre-spot, 000 , of the pattern. It is parallel to the normal of the reflecting plane, (hkl) . The magnitude of R_{hkl} is inversely proportional to the interplanar spacing, d_{hkl} , of the diffracting plane, (hkl) (see References [\[4\]](#) to [\[9\]](#)). In the context of this document, vectors $\mathbf{R}_{h_1k_1l_1}$, $\mathbf{R}_{h_2k_2l_2}$, $(\mathbf{R}_{h_2k_2l_2} - \mathbf{R}_{h_1k_1l_1})$ and $(\mathbf{R}_{h_1k_1l_1} + \mathbf{R}_{h_2k_2l_2})$ are simplified as \mathbf{R}_1 , \mathbf{R}_2 , \mathbf{R}_{2-1} and \mathbf{R}_{1+2} respectively. The included angle between vectors, \mathbf{R}_1 and \mathbf{R}_2 , is denoted by γ^* . The basic parallelogram is

defined by \mathbf{R}_1 and \mathbf{R}_2 , where they are the shortest and next shortest in the pattern respectively and not along a common line. The spot, $h_2k_2l_2$, is positioned anticlockwise around the centre spot relative to spot, $h_1k_1l_1$.

Because the centre-spot is often very bright, it is often difficult to determine the exact centre of the pattern. Therefore, a practical procedure is to establish the magnitude of $|\mathbf{R}_{hkl}|$ by measuring the distance between the spots, hkl and $\bar{h}\bar{k}\bar{l}$ on the diffraction pattern and dividing by two, i.e.

$|\mathbf{R}_{hkl}| = \frac{1}{2}(|\mathbf{R}_{hkl}| + |\mathbf{R}_{\bar{h}\bar{k}\bar{l}}|)$. On the example pattern shown in [Figure 2](#), the magnitude of \mathbf{R}_1 , \mathbf{R}_2 and \mathbf{R}_{2-1} is obtained from $\frac{1}{2}(\mathbf{R}_1 + \bar{\mathbf{R}}_1)$, $\frac{1}{2}(\mathbf{R}_2 + \bar{\mathbf{R}}_2)$ and $\frac{1}{2}(\mathbf{R}_{2-1} + \bar{\mathbf{R}}_{2-1})$ respectively.



Key

\mathbf{R}_1 is the vector from 000 to spot, $h_1k_1l_1$, the shortest vector in the diffraction pattern

\mathbf{R}_2 is the vector from 000 to spot, $h_2k_2l_2$, the next shortest vector

NOTE The basic parallelogram is constituted by \mathbf{R}_1 and \mathbf{R}_2 .

Figure 2 — Example of the spot diffraction pattern from a single crystal

The relationship between the interplanar spacing, d_{hkl} , and the magnitude of R_{hkl} for a reflecting plane, (hkl) , can be approximately expressed as shown in [Formula \(1\)](#) (see References [7] and [8]):

$$L\lambda = R_{hkl} \times d_{hkl} \left[1 - \frac{3}{8} \left(\frac{R_{hkl}}{L} \right)^2 \right] = R_{hkl} \times d_{hkl} (1 - \Delta) \quad (1)$$

where

Δ is equal to $\frac{3}{8} \left(\frac{R_{hkl}}{L} \right)^2$;

L is the diffraction camera length and equal to $f_o \times M_i \times M_p$;

where

f_o is the focal length, in millimetres, of the objective lens in the microscope;

M_i is the magnification of the intermediate lens;

M_p is the magnification of the projector lenses;

- $L\lambda$ is the camera constant (or diffraction constant) of the transmission electron microscope operating under the particular set of conditions. This parameter can be determined from the diffraction pattern of a crystalline specimen of known lattice parameters (see 8.3);
- λ is the wavelength, in nanometres, of the incident electron beam which is dependent upon the accelerating voltage and can be given by Formula (2) (see Reference [4]):

$$\lambda(\text{nm}) = \frac{1,226}{\sqrt{V(1+0,9788 \times 10^{-6}V)}} \quad (2)$$

where V is the accelerating voltage, in volts, of the TEM; the factor in parenthesis is the relativistic correction.

For most work using a TEM, the value of Δ in Formula (1) is usually smaller than 0,1 % and, hence, a more simplified Formula (3) may be used:

$$R_{hkl} \times d_{hkl} \cong L\lambda \quad (3)$$

For the derivation of the above equation, refer to the textbooks (see References [4] to [9]).

The use of Formula (3) requires measuring the length of R_{hkl} . Since, as mentioned earlier, the location of the pattern centre may not be easily determined; it is recommended that the distance measurement taken, $2R_{h_1k_1l_1}$, be from the $h_1k_1l_1$ diffracted spot to the $\bar{h}_1\bar{k}_1\bar{l}_1$ spot on the pattern. This is equivalent to a diameter measurement on the ring pattern from a polycrystalline specimen (Section 4.4 and Figure 4). To obtain the interplanar information, the measured distance, $2R_{h_1k_1l_1}$, is halved and Formula (3) applied.

If the camera constant is known, the interplanar spacing, d_{hkl} , of plane, (hkl) , can be calculated. The included angle between any two vectors, $R_{h_1k_1l_1}$ and $R_{h_2k_2l_2}$, can also be measured on the diffraction pattern. This is equal to the angle between the corresponding crystallographic planes, $(h_1k_1l_1)$ and $(h_2k_2l_2)$.

Since diffraction data from a single pattern will provide information on a limited number of the possible diffracting planes in a specimen area, it is necessary to acquire additional diffraction patterns from the same area (or from different grains/particles of the same phase). This requires either the tilting of the specimen or the availability of differently oriented grains or particles of the same phase.

Acquire a second diffraction pattern from another zone axis from the same area by tilting (or tilting and rotating) the specimen so that the two patterns contain a common spot row (see 8.2.11 and Figure 5). Index the diffracted spots, and then select three non-coplanar spots in the two patterns to constitute a reciprocal lattice, which, if the spots correspond to low values of Miller indices, may define the primitive unit cell of the crystal lattice. Therefore, crystal lattice parameters can be determined and the orientation of the grain or particle in the thin specimen can also be calculated.

4.3 Kikuchi pattern

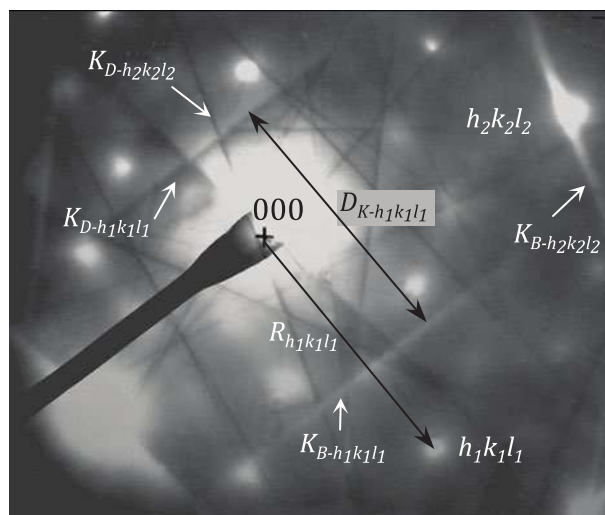
When a specimen area is nearly perfect but not thin enough, Kikuchi lines may occur. They arise from electrons scattered inelastically through a small angle and suffering only a very small energy loss being scattered again, this time elastically. This process leads to local variations of the background intensity in the diffraction pattern and the appearance of Kikuchi lines.

The Kikuchi patterns consist of pairs of parallel bright and dark lines, which are parallel to the projection of the corresponding reflecting plane, (hkl) . The bright (excess) line and dark (defect) line in the Kikuchi pattern are denoted by K_{B-hkl} and K_{D-hkl} , respectively. Therefore, the line pair, K_{B-hkl} and K_{D-hkl} , will be perpendicular to the vector, R_{hkl} , from the corresponding crystallographic plane (hkl) . Namely they are perpendicular to the reciprocal vector, g_{hkl} , of the plane, (hkl) .

An example of the Kikuchi patterns is given in Figure 3, where the bright line, K_{B-hkl} , and dark line, K_{D-hkl} , pairs are superimposed on the spot pattern. The perpendicular distance, $D_{K-h_1k_1l_1}$, between the line pair,

$K_{B-h_1k_1l_1}$ and $K_{D-h_1k_1l_1}$, is related to the interplanar spacing, $d_{h_1k_1l_1}$, and camera constant, $L\lambda$, by [Formula \(4\)](#).

$$D_{K-hkl} \times d_{hkl} \cong L\lambda \quad (4)$$



Key

K_{B-hkl}	bright line of Kikuchi pair
K_{D-hkl}	dark line of Kikuchi pair
$D_{K-h_1k_1l_1}$	distance between the line pair $K_{B-h_1k_1l_1}$ and $K_{D-h_1k_1l_1}$
+	centre of the direct beam

Figure 3 — Kikuchi pattern from a steel specimen

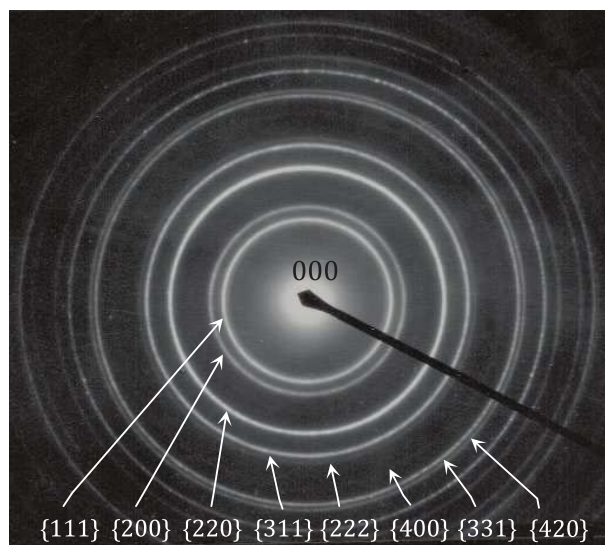
The distance between the two Kikuchi lines equals to the distance between the diffraction spot, hkl , and the central spot, 000. The angles between intersecting Kikuchi pairs are the same as the angles between the R_{hkl} vectors of their corresponding diffraction spots, and can be measured accurately. These angles are also equal to the angles between the relevant crystallographic planes.

When the specimen is tilted, the diffraction spots only gradually change the brightness, faint or increase the intensity, but their position change is hard to distinguish. Instead, Kikuchi lines are sensitive to the tilting. Their movement is significant on the viewing screen. Hence, specimen tilting can be guided by Kikuchi map from one zone axes to another one. The Kikuchi patterns present the real crystal symmetry of the specimen. They can also be used in establishing crystal orientation with a very high accuracy (see References [4] and [9]).

The problem is that Kikuchi patterns cannot always be observed in all of the specimens. In most cases, the SAED studies rely mainly on the spot patterns, though they are not as accurate as Kikuchi patterns.

4.4 Diffraction pattern of polycrystalline specimen

For randomly oriented aggregates of polycrystals, the diffraction pattern is comprised of a series of concentric rings centred on the spot, 000, of the direct beam. An example of the pattern from polycrystalline gold (Au) specimen is given in [Figure 4](#). Each diffracted ring arises from the diffraction beams from differently oriented crystallographic planes of the form, $\{hkl\}$; each of these having an identical interplanar spacing. From the diameter of each diffraction ring, the corresponding interplanar spacing, d_{hkl} , can be calculated using [Formula \(3\)](#). Indices of the diffraction rings can be ascribed and then the lattice parameters can also be determined. For the method of indexing ring patterns, refer to that used in X-ray powder diffraction (see Reference [9]).



NOTE Au possesses a face-centred cubic (FCC) structure with lattice parameter $a = 0,407\ 8\ \text{nm}$

Figure 4 — Diffraction ring pattern with indices from a polycrystalline Au specimen

5 Reference materials

A reference specimen is required for determining the diffraction constant, $L\lambda$, of the microscope in electron diffraction studies. In principle, any thin crystalline foil or powder can be considered as the reference specimen, provided its crystalline structure and lattice parameters have been acquired accurately and they are certified and stable under irradiation of the electron beam. It should be ensured that the reference material, which is as thin as electrons can penetrate through it, has the same crystallographic properties as the bulk material. In addition, a number of sharp diffraction rings or spots with known indices can be observed. The thickness of the crystal foil or powder grain size should be consistent with the beam energy and the quality of the diffraction pattern so that clear diffraction patterns can be observed (when it is too thick, the pattern will lack sharpness).

Reference materials in common use are polycrystalline specimens made from pure gold (Au) [which has a face-centred cubic (FCC) lattice with parameter, $a = 0,407\ 8\ \text{nm}$] or pure aluminium (Al) (FCC structure with lattice parameter $a = 0,404\ 9\ \text{nm}$). The mass fraction of Au or Al in the reference materials shall be not less than 99,9 %. The reference specimen shall be prepared by evaporating a small piece of Au or Al on a grid with a supporting film.

It is also feasible to evaporate a layer of the reference material onto a local surface area of the specimen, which is to be analysed.

6 Apparatus

6.1 Transmission electron microscope (TEM)

The TEM shall be equipped with double tilt or tilt rotation or double-tilt rotate specimen holder.

6.2 Recording of SAED patterns and images

The SAED patterns and images obtained on the transmission electron microscope shall be recorded on the photographic films or imaging plates or an image sensor built in the digital camera.

When films are used, a darkroom with a negative developing and fixing outfit is required.

7 Preparation of specimens

7.1 Most specimens are prepared as thin foils (see References [2], [10] and [11]). Such specimens can be obtained in the form of thin sections from a variety of crystalline substances including metallic and non-metallic materials. The shape and external size of the specimen should match that of the TEM specimen holder or, alternatively, it can be held by a support grid.

Fine powders and/or extraction replicas can also be used. These specimens shall be prepared on the grid with supporting films.

7.2 An applicable area to be tested is in the sizes of micrometre or sub-micrometre. The area is always defined by selected area (selector) aperture. The selected area shall be thin enough for the electron beam to pass through it and diffraction patterns can be observed on the viewing screen.

7.3 The surface of the specimen shall be clean, dry and flat without an oxidizing layer or any contamination.

7.4 For those materials that are stable under energetic particle beam bombardment, contamination on the specimen surface can be avoided or removed by ion beam sputtering or other techniques, such as plasma cleaners, before the TEM observation.

7.5 Prepared specimens should be labelled and placed in a special specimen box and preserved in a desiccator or evacuated container.

8 Procedure

8.1 Instrument preparation

8.1.1 The general working condition of the TEM laboratory should comply with ISO/IEC 17025 (see Reference [1]).

8.1.2 It is recommended to use the cold trap of TEM before conditioning in order to minimize specimen contamination.

8.1.3 When the vacuum of the transmission electron microscope is suitable for operation, switch on and select an appropriate accelerating voltage so that the incident electron beam can penetrate through the specimen.

8.1.4 Carry out the axis alignment for the electron optical system.

8.1.5 The success of the selected area electron diffraction method relies on the validity of indexing the diffraction patterns arising, irrespective of which axis in the specimen lies parallel to the incident electron beam. Such analysis is therefore aided by specimen tilt and rotation facilities.

Place the specimen to be tested and the reference firmly in the double-tilting or tilting-rotation or double-tilting rotation specimen holder, and insert the holder into the specimen chamber.

A specimen coated with an evaporated layer of reference material can be directly placed in the specimen holder and inserted into the chamber.

8.1.6 When the SAED patterns need to be related to features observed in the corresponding micrograph, the angle of rotation between the two may need to be determined and compensated for.

The method in common use is to take a diffraction pattern and a micrograph of a molybdenum trioxide crystal specimen. The rotation angle of the image is then measured on the photographic plates or digital

images, on which the micrograph and superimposed diffraction pattern has been recorded. For details of the calibration procedure, refer to the appropriate text books (see References [4], [5] and [9]).

When the rotation angle of the TEM has been compensated by the manufacturer, the procedure in 8.1.6 may be ignored.

8.1.7 When a digital camera is equipped and to be employed for the study, set the camera in operating condition by following the user's guide of the manufacturer.

To avoid damaging the camera, reduce incident beam intensity and use beam stop to block the central spot when acquiring SAED diffraction patterns.

For detail procedure of the operation and calibration, refer to instruction from the manufacturer.

8.2 Procedure for acquiring SAED patterns from a single crystal

8.2.1 Obtain a magnified bright field image of the specimen on the viewing screen of the transmission electron microscope. Adjust the specimen height to focus the image so that the image movement is minimized during the tilting of the specimen. Namely, set the eucentric position of the specimen. The procedure for establishing the eucentric position of the specimen may be obtained by consulting the manufacturer's operating manual.

NOTE If the TEM is not equipped with a specimen height control function, this procedure can be omitted.

8.2.2 Adjust the magnification of the specimen image until details in the specimen can be observed clearly. A suitable magnification for SAED analysis is usually from several thousands to tens of thousands times. Focus the image and correct the astigmatism.

8.2.3 Insert the selected area (selector) aperture and focus the image of this aperture. Then, focus the specimen image again. This makes the selected area (selector) aperture plane conjugate with the image plane of the objective lens.

8.2.4 Switch the microscope from image mode to the SAED mode, focus the image of the objective lens aperture; that is, make this objective lens aperture coincide with the back focal plane of the objective lens. Return to the bright field image mode and focus the image again.

8.2.5 Insert the reference (i.e. the calibration standard) and locate it at the eucentric position. Choose a camera length, L , consistent with the capabilities of the subsequent measuring equipment and then obtain a diffraction pattern from it. Focus the diffraction pattern and correct any astigmatism carefully to make the diffraction pattern sharp. Record the diffraction pattern of the reference.

8.2.6 If the reference and test specimen are not in the same specimen holder, withdraw the reference and insert the test specimen again, without changing the operating conditions and without switching the microscope off. Again, locate it at the eucentric height.

8.2.7 Obtain a focused bright field image of the specimen again with an appropriate magnification. Select a region of interest (ROI) on the specimen image using the selected area (selector) aperture. Record the image of this ROI in the specimen. The phase boundaries and/or grain boundaries in the specimen should be kept away from the selected ROI when a single crystal grain is analysed.

8.2.8 Switch the TEM to the SAED diffraction mode again, withdraw the objective lens aperture and obtain a diffraction pattern on the viewing screen. Where possible, tilt the specimen slightly so that the brightness

of the spots in the diffraction pattern is evenly distributed, or where Kikuchi lines appear; the Kikuchi line pairs are symmetrical about the pattern centre.

This pattern will then derive from a low index direction in the crystal approximately; the direction is antiparallel to the incident electron beam. This crystal direction will be the zone axis, $[u_1v_1w_1]$, which is the normal of the reciprocal plane, $(u_1v_1w_1)^*$, i.e. the diffraction pattern (see References [4] to [7]).

NOTE The beam direction is defined as antiparallel to the incident electron beam.

Adjust (defocus) the second condenser lens current (the brightness knob) to sharpen the diffraction spots, making them as sharp as possible.

8.2.9 Record the pattern or/and save the original uncompressed pattern in the computer system. Take note of the reading on the X and Y axis of the specimen tilting device as X_1 and Y_1 , respectively. Using dark field conditions either by beam tilt or shifting the objective lens aperture, identify the source of the pattern.

8.2.10 Insert the reference specimen and obtain a second diffraction pattern from the reference. Record this diffraction pattern (see also 8.3), making sure that the same experimental conditions are used (i.e. accelerating voltage, lens settings and, especially, the specimen height and camera length, L).

NOTE Polycrystalline reference or specimens need not be tilted to achieve a specific zone axis orientation.

8.2.11 Obtain sufficient data for each phase of interest by either of the following procedures.

a) Specimen tilting procedure: obtain the second pattern by tilting the specimen.

Choose a row of close-spaced diffraction spots collinear with the central transmitted spot on the diffraction pattern, which is denoted by indices of reciprocal plane, $(u_1v_1w_1)^*$. Keep this row of the spots visible on the viewing screen, while tilting the specimen until the second diffraction pattern, $(u_2v_2w_2)^*$ appears. Make sure the brightness of the spots in the second pattern is evenly distributed. The reciprocal space geometry of the two patterns is schematically illustrated in Figure 5. The angle between the diffraction patterns, $(u_1v_1w_1)^*$ and $(u_2v_2w_2)^*$, is ψ , which equals to the angle between the two zone axes, $[u_1v_1w_1]$ and $[u_2v_2w_2]$. This angle can be determined from the tilt angle of the specimen holder.

If Kikuchi patterns are visible, the specimen tilting can be guided by the Kikuchi map. The second diffraction pattern (or more patterns) may be obtained directly.

With a rotate-tilt specimen holder or a double-tilting rotate holder, a chosen row of the spots can be aligned with a tilt axis; the second diffraction pattern (or more patterns) may be obtained directly.

Repeat the procedure described in 8.2.8, recording the pattern and/or saving it on the computer system. Take note of the reading on the X and Y axis of the specimen-tilting device as X_2 and Y_2 , respectively.

b) Multi grains procedure: obtain the patterns from several areas, i.e. different particles or grains of the same phase. This procedure is recommended for any of the following situations:

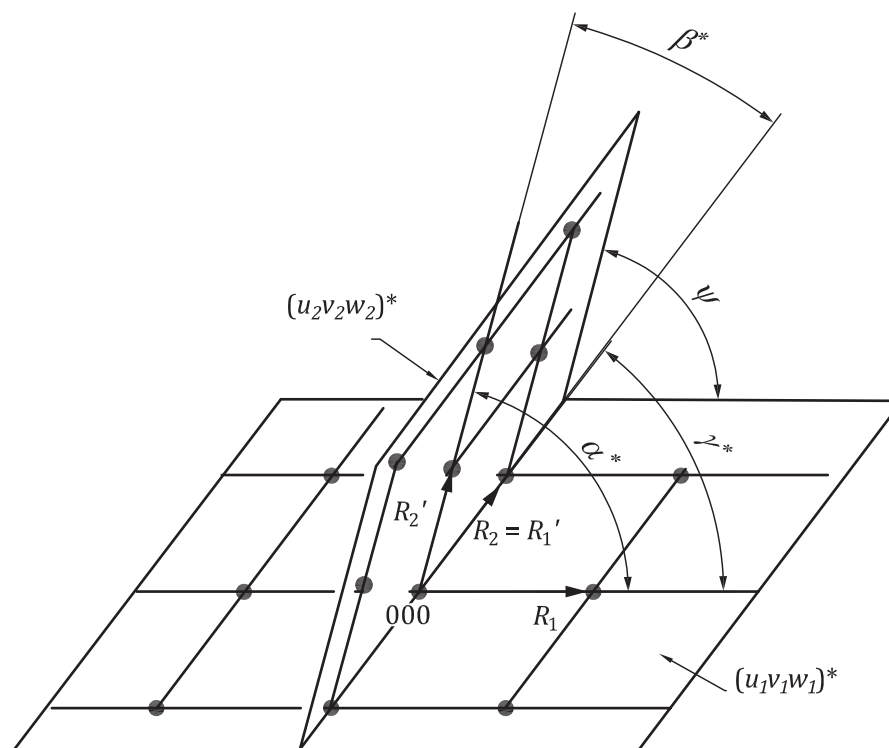
- 1) the maximum tilting angle of the specimen holder is not large enough, so that the second diffraction pattern cannot be reached by tilting;
- 2) the particles to be analysed in the specimen are too small;
- 3) the specimen is sensitive to the electron beam illumination, e.g. the selective area is contaminated or decomposes following a short irradiation by the electron beam.

When this procedure is employed, the source of each diffraction pattern is necessary to confirm. Choose appropriate diffraction spots to form a dark field image to check it. Further confirmation can be achieved through simultaneous use of EDS (energy dispersive X-ray spectrometry) facility, when available.

8.2.12 When the diffraction patterns are recorded on negative films, develop, fix and dry the films in the darkroom. Keep the negative films one by one in individual protective bags with labels.

8.2.13 When the diffraction patterns are recorded by digital camera or imaging plates, save the original uncompressed diffraction patterns in the computer system as individual files with labels. All parameters of the acquisition of this file shall be documented and reported.

8.2.14 Each pattern, either recorded on negative film or by digital camera as well as by imaging plate, shall be numbered and labelled with the following information: specimen designation and serial number, accelerating voltage, nominal camera length, L , tilting angles, operator, date, etc. All processing operations on the diffraction patterns and images shall be reported



Key

ψ is the angle between the diffraction pattern $(u_1 v_1 w_1)^*$ and $(u_2 v_2 w_2)^*$

$$R_1' = R_2$$

Figure 5 — Reciprocal space geometry of the spot diffraction patterns

8.3 Determination of diffraction constant, $L\lambda$

8.3.1 The procedure for the determination of the diffraction constant, $L\lambda$, uses a reference specimen such as polycrystalline pure gold or pure aluminium (see [Clause 5](#)). [Figure 4](#) shows an example of the ring patterns from a polycrystalline gold specimen. Record the diffraction pattern (see [8.2](#)).

8.3.2 When diffraction patterns are recorded on photographic films, place the negative film on which the diffraction pattern of the reference specimen was recorded, emulsion side up on the film viewer. Measure the diameters of the diffraction rings on the film of the reference specimen when a polycrystalline reference is used. Note the diameter of these rings from inner to outer as $D_1, D_2, D_3, D_4, \dots$ (mm), etc., respectively.

When the diffraction patterns are recorded by the digital camera, the above measurement is carried out on the computer system.

8.3.3 Indices, hkl , of the diffraction rings for a reference specimen with FCC structure are 111, 200, 220, 311, 222, 400, 331, 420, 422, ... respectively from the inner to outer rings (see [Figure 4](#)). The corresponding interplanar spacings, d_{hkl} , are given for both Au and Al in [Annex A](#) or calculated by the crystallographic formulae (see References [4] to [9]).

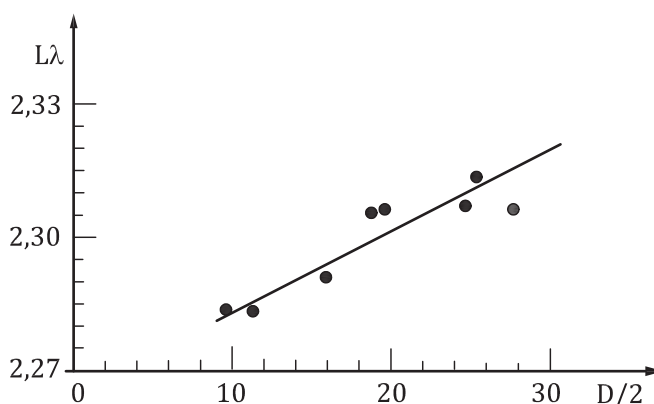
8.3.4 According to [Formula \(3\)](#), calculate the diffraction constants as follows:

$$\begin{aligned} L_1\lambda &= D_1 \cdot d_{111} / 2 & (\text{mm} \cdot \text{nm}) \\ L_2\lambda &= D_2 \cdot d_{200} / 2 & (\text{mm} \cdot \text{nm}) \\ L_3\lambda &= D_3 \cdot d_{220} / 2 & (\text{mm} \cdot \text{nm}) \dots, \text{etc.} \end{aligned}$$

where

d_{111} , d_{200} and d_{220} is the interplanar spacing of the crystallographic plane {111}, {200} and {220} of the specimen respectively;

D_1 , D_2 and D_3 is the diameter of diffracted ring {111}, {200} and {220} of the specimen respectively, on the ring pattern of the specimen.



Key

$D/2$ is one- half diameter of a diffracted ring, expressed in mm

$L\lambda$ is the diffraction constant, expressed in mm·nm

Figure 6 — $L\lambda \sim D/2$ curve from a polycrystalline Au specimen

8.3.5 Plot the $L\lambda \sim D/2$ curve using the data in [8.3.2](#) and [8.3.4](#) (an example of the $L\lambda \sim D/2$ plot is shown in [Figure 6](#)). This graph can be used for all reflections (spots) from the specimen being analysed under completely identical conditions. Since the diffraction constant, $L\lambda$, actually varies slightly with the diffraction ring diameter, it is recommended to either:

- use the $L\lambda \sim D/2$ curve to obtain the value of $L\lambda$ corresponding to the same distance, $D/2$, as the spot being measured;
- use an average value of the camera constant and subsequently make allowance for the small uncertainty this will produce in the d -value obtained.

9 Measurement and solution of the SAED patterns

9.1 Selection of the basic parallelogram

9.1.1 When photographic films are used for recording diffraction patterns, place the film, on which the diffraction pattern was recorded, on the film viewer with its emulsion side up.

When the digital camera is used for recording diffraction patterns, open the file on the computer.

9.1.2 Select two diffracted spots, $h_1k_1l_1$ and $h_2k_2l_2$, from the diffraction pattern with zone axis, $[u_1v_1w_1]$, such that these spots are the nearest and next nearest to the central spot, 000, respectively. They shall not be collinear with the centre-spot, 000. The spot, $h_2k_2l_2$, is positioned anticlockwise around the centre spot relative to spot, $h_1k_1l_1$. The two diffracted spots, the centre-spot and the spot, $(h_1 + h_2, k_1 + k_2, l_1 + l_2)$, constitute a parallelogram (see [Figure 2](#)).

Measure the distance, $2R_1$ between the spots, $h_1k_1l_1$ and $\bar{h}_1\bar{k}_1\bar{l}_1$, and the distance, $2R_2$, between the spots, $h_2k_2l_2$ and $\bar{h}_2\bar{k}_2\bar{l}_2$, to get the magnitude of the vectors, \mathbf{R}_1 and \mathbf{R}_2 (see [Figure 2](#)). The corresponding angle, γ^* , between \mathbf{R}_1 and \mathbf{R}_2 shall also be measured.

Where individual patterns are obtained, obtain the magnitude of the vectors, \mathbf{R}_{1+2} and \mathbf{R}_{2-1} (see [Figure 2](#)). The angles between $\bar{\mathbf{R}}_1$ and \mathbf{R}_{2-1} , between \mathbf{R}_{2-1} and \mathbf{R}_2 as well as the angle between $\bar{\mathbf{R}}_1$ and \mathbf{R}_2 shall be measured. These are ϕ_3 , ϕ_2 and ϕ_1 respectively, and $\phi_3 + \phi_2 = \phi_1$.

9.1.3 The angles ϕ_3 , ϕ_2 and ϕ_1 can be calculated using [Formulae \(5\)](#), [\(6\)](#) and [\(7\)](#):

$$\phi_1 = \cos^{-1} \left[\left(R_1^2 + R_2^2 - R_{1+2}^2 \right) / 2R_1R_2 \right] \quad (5)$$

$$\phi_2 = \cos^{-1} \left[\left(R_2^2 + R_{2-1}^2 - R_1^2 \right) / 2R_2R_{2-1} \right] \quad (6)$$

$$\phi_3 = \cos^{-1} \left[\left(4R_1^2 + R_{2-1}^2 - R_{1+2}^2 \right) / 4R_1R_{2-1} \right] \quad (7)$$

If $\phi_1 = \phi_2 + \phi_3$ is within the tolerances set by the uncertainty, then proceed; otherwise, check \mathbf{R}_S and ϕ_S .

9.1.4 Perform the same procedure as described in [9.1.3](#) on the second diffraction pattern with zone axis, $[u_2v_2w_2]$ (and on any others from different directions of the specimen). The basic parallelogram on the second pattern is constituted by \mathbf{R}'_1 , \mathbf{R}'_2 and the centre-spot, 000. The vector, \mathbf{R}'_1 , shall be superimposed over the vector, \mathbf{R}_2 , of the pattern with zone axis, $[u_1v_1w_1]$, i.e. $\mathbf{R}'_1 = \mathbf{R}_2$ (see [Figure 5](#)). Measure the magnitude of \mathbf{R}'_1 and \mathbf{R}'_2 as well as the angle, β^* , between \mathbf{R}'_1 and \mathbf{R}'_2 . The vectors, \mathbf{R}_1 , \mathbf{R}_2 and \mathbf{R}'_2 constitute a basic cell of the reciprocal space. If the corresponding diffraction spots possess the lowest indices, then the reciprocal unit cell can be obtained.

9.1.5 When a digital camera is employed, measurement and calculation on the diffraction patterns can be carried out by the computer system.

9.1.6 The angle, α^* , between R_1 and R_2' (see [Figure 5](#)) may be calculated using [Formula \(8\)](#):

$$\cos \alpha^* = \sin \gamma^* \times \sin \beta^* \times \cos \psi + \cos \gamma^* \times \cos \beta^* \quad (8)$$

where

β^* is the angle between R_1' and R_2' ;

γ^* is the angle between R_1 and R_2 ;

ψ is the angle between the diffraction patterns, $(u_1 v_1 w_1)^*$ and $(u_2 v_2 w_2)^*$, or the zone axes, $[u_1 v_1 w_1]$ and $[u_2 v_2 w_2]$.

9.2 Indexing diffraction spots

9.2.1 Use [Formula \(3\)](#) to calculate the interplanar spacing, d_{hkl} , corresponding to the above diffraction spots. The interplanar spacing, d_{hkl} , can also be acquired by measuring the distance, D_{K-hkl} , between the Kikuchi bright and dark line pair and using [Formula \(4\)](#).

9.2.2 Arbitrarily index two of the spots, say $(h_1 k_1 l_1)$ and $(h_2 k_2 l_2)$, provided that the interplanar spacing of the planes is consistent with their calculated value, and then confirm from the possible indices of the other spots that:

$$h_3 = h_2 - h_1, k_3 = k_2 - k_1, l_3 = l_2 - l_1, \text{ and}$$

$$h_4 = h_2 + h_1, k_4 = k_2 + k_1, l_4 = l_2 + l_1$$

Make any allowance for the multiplicity of $\{h_j k_j l_j\}$. If no solution is possible, then recheck the determination of d_i and the angles (see [9.1.3](#)) until one is found that satisfies these requirements within the tolerances. All spots in a continuous pattern will come from a common zone, $[uvw]$, and have a common axis. This direction is given by [Formula \(9\)](#). The direction, $[uvw]$, can be checked since for all (hkl) 's indexed

$$hu + kv + lw = 0 \quad (9)$$

9.2.3 Calculate the characteristic parameters of the two-dimensional primitive cell on each reciprocal lattice plane of the crystal specimen in advance, namely the indices, $h_1 k_1 l_1$ and $h_2 k_2 l_2$, of the primitive reciprocal vector, \mathbf{g}_1 and \mathbf{g}_2 , ratio of the magnitudes, $g_2 : g_1$, the included angle between the vectors \mathbf{g}_1 and \mathbf{g}_2 as well as the zone axis index.

The zone axis index, $[uvw]$, can be obtained using [Formula \(10\)](#):

$$u:v:w = \left[\begin{array}{c|c|c} k_1 & l_1 & h_1 \\ k_2 & l_2 & h_2 \end{array} \right] = [(k_1 l_2 - l_1 k_2) : (l_1 h_2 - h_1 l_2) : (h_1 k_2 - k_1 h_2)] \quad (10)$$

The values of u, v, w should be integers without a common factor. If the indices u, v and w contain a common integral factor n , divide them by the common factor n . The zone axis index, $[uvw]$, can also be converted to the reciprocal index by the crystallographic relation. The formulae for the index conversion may be obtained from literature and/or handbooks (such as References [\[4\]](#), [\[5\]](#), [\[6\]](#), [\[7\]](#) and [\[9\]](#)).

For the convenience of users of this document, the standard spot patterns of cubic systems and close-packed hexagonal system with low indices are given in [Annex B](#). For those specimens with a lower symmetry, it is recommended to refer to a diffraction database such as "The Powder Diffraction File", published by the International Centre for Diffraction Data (ICDD), (see Reference [\[12\]](#)). Software is also very useful in

establishing the reciprocal planes of the crystal specimen, especially in one with low symmetry structure (see References [4] and [9]).

For an unknown specimen, the chemical composition should also be determined by microanalysis (e.g. EDS analysis) and/or chemical analysis so that the specimen phase can be identified.

9.2.4 Compare the geometrical characteristics of the experimental diffraction patterns, including the ratio, R_2 / R_1 and R_{2-1} / R_1 , the included angle between R_1 , R_2 and R_{2-1} , respectively, with the calculated characteristic parameters of the primitive cell. If the experimental value is consistent with the known value within error, the diffraction spots can be indexed as $h_1 k_1 l_1$, $h_2 k_2 l_2$ and $(h_2 - h_1, k_2 - k_1, l_2 - l_1)$, respectively. The indices of other diffraction spots can be obtained by the summation of the corresponding vectors. Therefore, the zone axis index, $[uvw]$, can be worked out.

9.2.5 Computer programs may be used for indexing the diffraction patterns, so long as the diffraction constant has been appropriately calibrated within the software

9.2.6 For beam-sensitive nanocrystals, it is often incapable to collect a tilting series of the diffraction patterns from a single nanocrystal. The method that uses randomly oriented diffraction patterns with unknown angular relationships may apply. The key point of this approach is to construct a principal facet by the lengths of the two basis vectors and the angle between them in the diffraction pattern. Based on matching the observed crystal facets to model facets extracted from a simulated three-dimensional lattice, the potential unit cell can be determined. The diffraction pattern can also be indexed. For a detailed procedure of this algorithm, refer to References [13] and [14].

10 180° ambiguity

The indices in a diffraction pattern with only one zone axis from a single crystal are not decided uniquely because of the 180° ambiguity created by the diffraction effect. Therefore, the spots, $h_1 k_1 l_1$ and $h_2 k_2 l_2$, can also be indexed as $\bar{h}_1 \bar{k}_1 \bar{l}_1$ and $\bar{h}_2 \bar{k}_2 \bar{l}_2$, respectively, and vice versa, except that higher Laue zone diffraction spots can be obtained.

However, this ambiguity may be removed by the following methods.

- After recording a diffraction pattern, $[u_1 v_1 w_1]$, tilt the specimen while keeping a row of spots bright, containing the central spot, until another zone axis pattern, $[u_2 v_2 w_2]$, appears. Record the second pattern and determine the included angle between the two patterns (see 8.2.11). Index the two patterns so that all the indices are entirely self-consistent. The angle between the two patterns shall coincide with the tilting angle.
- Obtain a diffraction pattern with zone axis, $[u_1 v_1 w_1]$, which is superposed on another pattern, $[u_2 v_2 w_2]$, from the same crystal. Index the two patterns self consistently.
- Tilt the specimen to get three non-parallel Kikuchi line pairs in one pattern. Unambiguous indices can be gained.

11 Uncertainty estimation

11.1 General

The interplanar spacings d_{hkl} , i.e. d -spacings, of the specimen crystal are the essential results for a SAED study. The uncertainty in the d -spacings is affected by the following factors:

- $u(L)$: is the uncertainty in the camera length L ;
- $u(f_o)$: is the uncertainty in focal length f_o of the objective lens of the TEM;

- $u(\lambda)$: is the uncertainty in wavelength λ of the incident electron beam;
- $u(R_{hkl})$: is the uncertainty in determination of the spot spacings or ring diameters on the diffraction pattern.

11.2 Uncertainty in camera constant

The camera constant will change if the high voltage supply to the electron microscope fluctuates. Normally, stabilization ratios are 10^5 to 1 or better and thus, this effect is minimal. The uncertainty $u(\lambda)$ can be ignored. As discussed in [Clause 4.2](#), the effective camera length, L , is defined as [Formula \(11\)](#) (see Reference [7]):

$$L = f_o \times M_i \times M_p \quad (11)$$

where

- f_o is the focal length of the objective lens;
- M_i is the magnification of the intermediate lens;
- M_p is the magnification of the projector lens.

The focal length f_o is the most sensitive factor which affects the reproducibility of L . It depends on the plane of the object. The factors that control this are specimen holders of different length, support grids that are not flat, thick and buckled specimens, and the effects due to tilting the specimen. Faulty lens settings will alter $2L\lambda$ if the correct procedure for obtaining diffraction settings is not followed.

According to ISO/IEC Guide 98-3:2008 (see Reference [15]), the relative uncertainty of the camera length $u(L)/L$ is given by [Formula \(12\)](#):

$$\frac{u(L)}{L} = \sqrt{\left[\frac{u(f_o)}{f_o}\right]^2 + \left[\frac{u(M_i)}{M_i}\right]^2 + \left[\frac{u(M_p)}{M_p}\right]^2} \quad (12)$$

where

- $u(M_i)$ is the uncertainty in the magnification of the intermediate lens;
- $u(M_p)$ is the uncertainty in the magnification of the projector lens.

In some instruments, the strength of the projector lens is fixed so that $u(M_p)/M_p = 0$. However, in other instruments, the projector current is variable and the accuracy of the setting has a marked effect on $2L\lambda$. The relative uncertainty $u(M_i)/M_i$ arises from re-adjusting the intermediate lens strength to image the diffraction pattern from the back focal plane of the objective lens. This adjustment can be made with considerable accuracy, so $u(M_i)/M_i$ is usually very small.

11.3 Calibration with a reference material

Measurement of d -spacings involves the use of a reference material so that the camera constant, $2L\lambda$, can be determined and the effects of variation in microscope parameters can be ignored, provided the conditions for obtaining the diffraction pattern of the standard and unknown are identical. Thus, the main uncertainties involved in the determination of the camera constant, and consequently the d -spacing values, arise from inaccuracies in the measurement of diffraction ring diameters and/or spot spacings.

NOTE The identical condition means that the specimen height, the focusing for image and for diffraction pattern are not altered, also the specimen tilting angles are not changed during recording the diffraction patterns of the standard and unknown.

When a polycrystalline specimen with known lattice parameters (such as pure Au or Al) is used as reference material to obtain $L\lambda \sim D_s / 2$ curve by measuring the ring diameters D_s of its diffraction pattern. The camera length, L , can be determined from this calibration curve. The uncertainty $u(D_s)$ in the ring diameters D_s can be expressed as [Formula \(13\)](#) :

$$u(D_s) = \sqrt{\frac{1}{n(n-1)} \sum_{i=1}^n (D_{si} - \bar{D}_s)^2} \quad (13)$$

where

D_s is the individual measured value of a ring diameter on the diffraction pattern of the reference;

\bar{D}_s is the arithmetic mean of n independent measurements on a ring diameter;

n is an integer.

Lens aberration may lead to distortion of diffraction rings into ellipses and thus, measurements of diameter shall be made at least n positions, ($n \geq 3$, it is recommended to take $n = 6$), when determining the $L\lambda \sim D_s / 2$ curve to determine the minimum and maximum values of the diameters (see [8.3.5](#)).

The camera length L_s obtained by the reference material is as follows:

$$L_s = D_{shkl} \times d_{shkl} / 2\lambda$$

Both of the uncertainty in wavelength λ of the incident beam and in d -spacings of the reference, d_{shkl} , are very small and can be ignored. The uncertainty in the camera length value, $u(L)$, is given by [Formula \(14\)](#):

$$u(L) = \frac{d_s}{2\lambda} \sqrt{\frac{1}{n(n-1)} \sum_{i=1}^n (D_{si} - \bar{D}_s)^2} \quad (14)$$

11.4 Uncertainty in d -spacing values

When [Formula \(3\)](#) is used to obtain d -spacing of the unknown specimen, the uncertainty involved in measurement of the spot spacings or ring diameters, $u(R_{hkl})$, can be estimated from replicate measurements of these values, thus:

$$u(R_{hkl}) = \sqrt{\frac{1}{m(m-1)} \sum_{j=1}^m (R_{hklj} - \bar{R}_{hkl})^2} \quad (15)$$

where

\bar{R}_{hkl} is the arithmetic mean of m independent measurements of a R_{hkl} vector or ring diameter on the diffraction pattern, $m \geq 3$ is recommended;

R_{hklj} is the j th individual measured magnitude of a R_{hkl} vector on the diffraction pattern of the specimen.

Note the magnitude of R_{hkl} is obtained by measuring the distance between the spots, hkl and \overline{hkl} on the diffraction pattern and dividing by two.

Thus, the uncertainty for determination of d -spacing values is combined by $u(L)$ and $u(R_{hkl})$, which is expressed by [Formula \(16\)](#).

$$u(d) = \sqrt{\left[\frac{\lambda}{R_{hkl}} \cdot u(L) \right]^2 + \left[\frac{L\lambda}{R_{hkl}^2} \cdot u(R_{hkl}) \right]^2} \quad (16)$$

The expanded uncertainty is: $U = k \cdot u(d)$.

where k is the coverage factor for a level of confidence of approximately 95 % set $k = 2$.

Annex A
(informative)

Interplanar spacings of references

A.1 Interplanar spacings of pure Au and Al

The interplanar spacings, d_{hkl} , of pure gold and aluminium are listed in [Table A.1](#).

Table A.1 — Interplanar spacing, d_{hkl} , of pure Au and Al

Dimensions in nanometres

Miller indices of crystallographic planes	Interplanar spacing of Au d_{hkl}	Interplanar spacing of Al d_{hkl}
{111}	0,235 50	0,233 80
{200}	0,203 90	0,202 40
{220}	0,144 20	0,143 10
{311}	0,123 00	0,122 10
{222}	0,117 74	0,116 90
{400}	0,101 96	0,101 24
{331}	0,093 58	0,092 89
{420}	0,091 20	0,090 55
{422}	0,083 25	0,082 66
{333}/{511}	0,078 00	—
NOTE 1 Lattice parameter for Au [face-centred cubic (FCC) structure, S.G: Fm3m(225)]: $a = 0,407\ 8\ \text{nm}$. See Reference [16] .		
NOTE 2 Lattice parameter for Al [FCC structure, S.G: Fm3m(225)]: $a = 0,404\ 9\ \text{nm}$. See Reference [16] .		

Annex B
(informative)

Spot diffraction patterns of single crystals for BCC, FCC and HCP structure [7]

B.1 Symbols and definitions

B.1.1 Zone axis, $[uvw]$

In a spot diffraction pattern, the symbol $[uvw]$ denotes index of the zone axis, which is the normal of this diffraction pattern.

B.1.2 Regulation for the reciprocal vectors

In this document, the symbols R_1 and R_2 in a spot diffraction pattern are specified as follows:

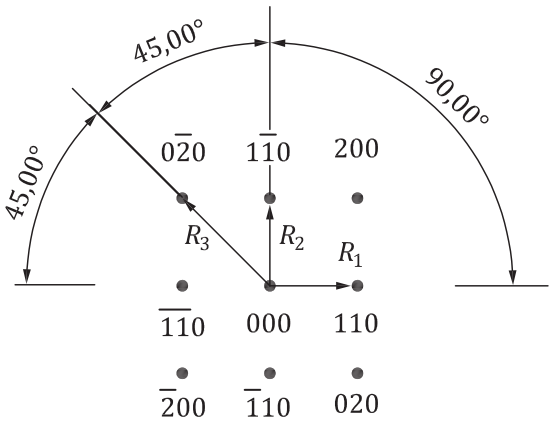
R_1 is the shortest vector in the diffraction pattern;

R_2 is the next shortest vector, which is not along a common line with R_1 and is positioned anticlockwise around the centre spot relative to R_1 . The relation between the vectors is as follows:

$R_3 = R_2 - R_1$ and $R_3 \geq R_2 \geq R_1$

B.2 Spot diffraction patterns for body-centred cubic (BCC) crystals

Spot diffraction patterns from a single crystal with BCC structure, for $(u^2+v^2+w^2) \leq 22$, are given in [Figures B.1](#) to [B.14](#).

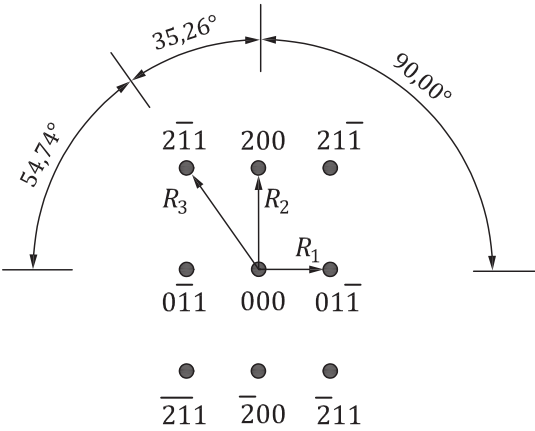


Key

$R_2/R_1 = 1,000$

$R_3/R_1 = 1,414$

Figure B.1 — $[uvw] = [001]$ for BCC

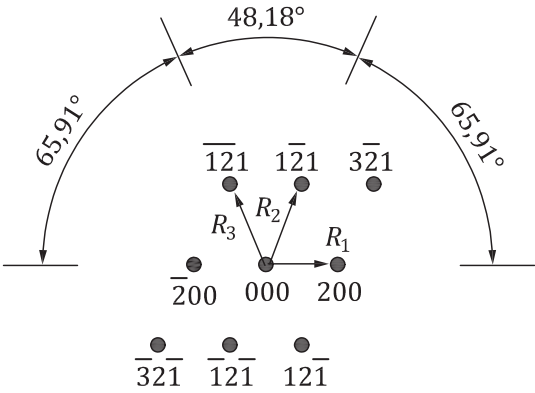


Key

$R_2/R_1 = 1,414$

$R_3/R_1 = 1,732$

Figure B.2 — $[uvw] = [011]$ for BCC

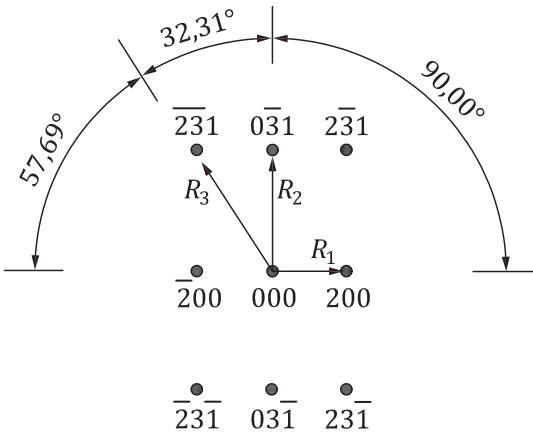


Key

$R_2/R_1 = 1,225$

$R_3/R_1 = 1,225$

Figure B.3 — $[uvw] = [012]$ for BCC

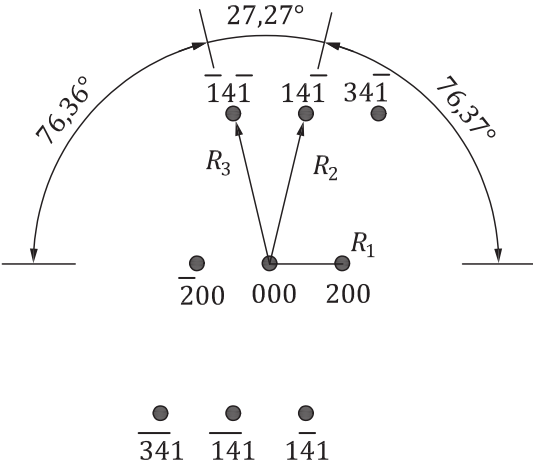


Key

$R_2/R_1 = 1,581$

$R_3/R_1 = 1,871$

Figure B.4 — $[uvw] = [013]$ for BCC



Key

$R_2/R_1 = 2,121$

$R_3/R_1 = 2,121$

Figure B.5 — $[uvw] = [014]$ for BCC

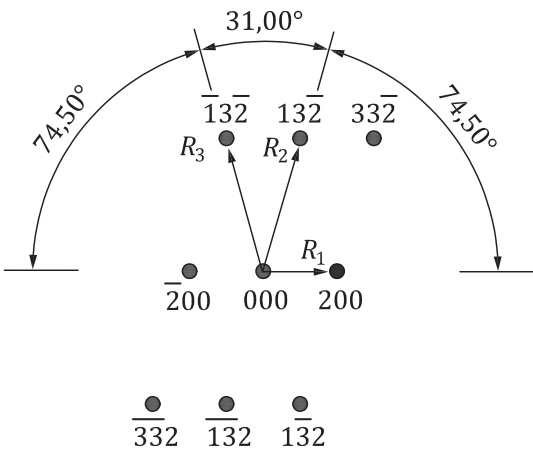


Figure B.6 — $[uvw] = [023]$ for BCC

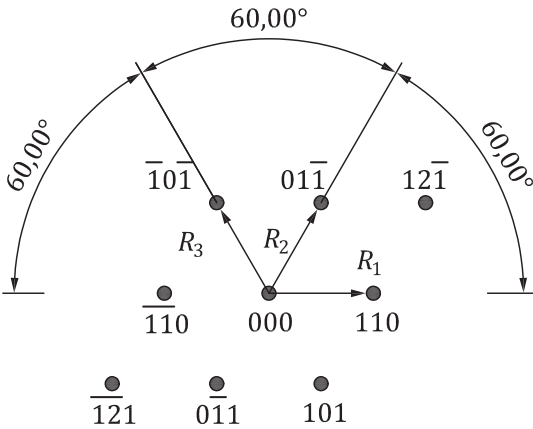
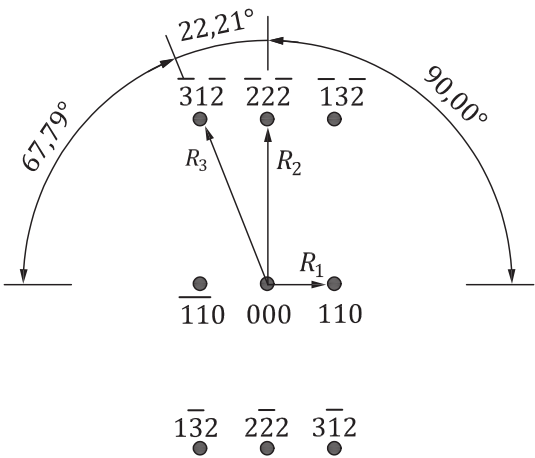


Figure B.7 — $[uvw] = [\bar{1}11]$ for BCC

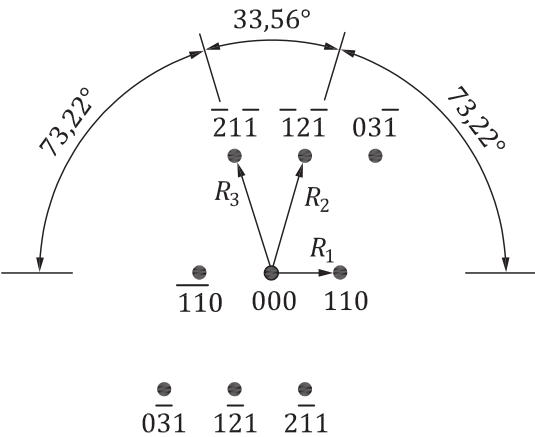


Key

$R_2/R_1 = 2,450$

$R_3/R_1 = 2,646$

Figure B.8 — $[uvw] = [\bar{1}12]$ for BCC

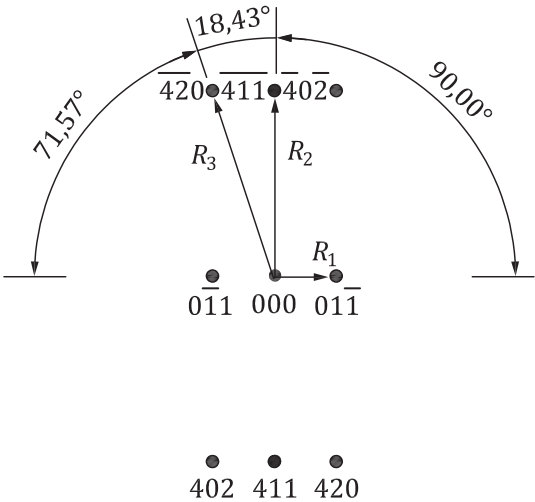


Key

$R_2/R_1 = 1,732$

$R_3/R_1 = 1,732$

Figure B.9 — $[uvw] = [\bar{1}13]$ for BCC

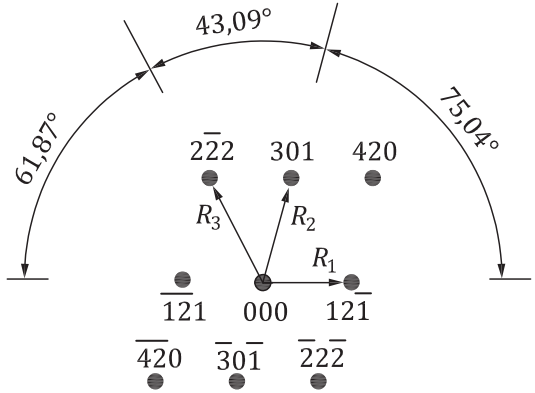


Key

$R_2/R_1 = 3,000$

$R_3/R_1 = 3,162$

Figure B.10 — $[uvw] = [\bar{1}22]$ for BCC

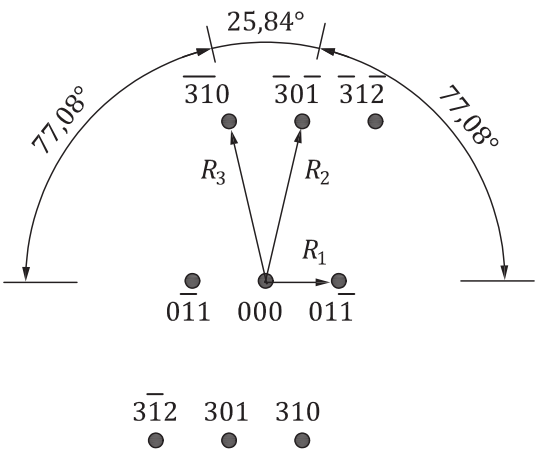


Key

$R_2/R_1 = 1,291$

$R_3/R_1 = 1,414$

Figure B.11 — $[uvw] = [\bar{1}23]$ for BCC

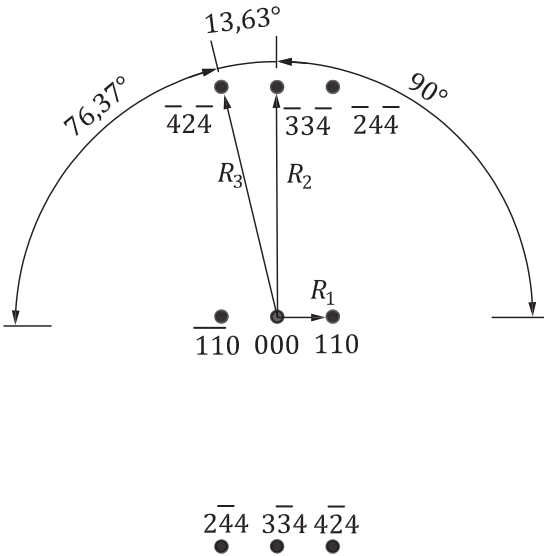


Key

$R_2/R_1 = 2,236$

$R_3/R_1 = 2,236$

Figure B.12 — $[uvw] = [\bar{1}33]$ for BCC

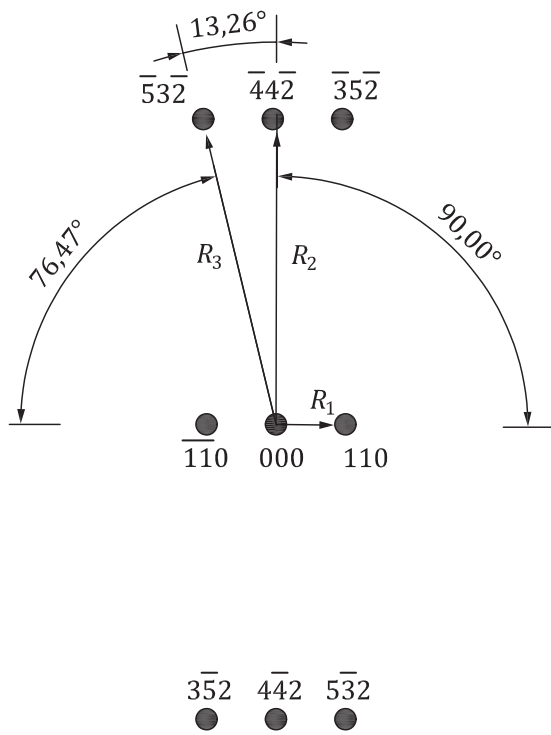


Key

$R_2/R_1 = 4,123$

$R_3/R_1 = 4,243$

Figure B.13 — $[uvw] = [\bar{2}23]$ for BCC



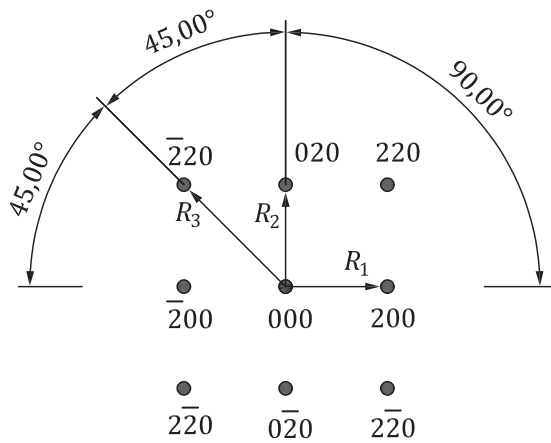
Key

$R_2/R_1 = 4,243$
 $R_3/R_1 = 4,359$

Figure B.14 — $[uvw] = [\bar{1}14]$ for BCC

B.3 Spot diffraction patterns for face-centred cubic (FCC) crystals

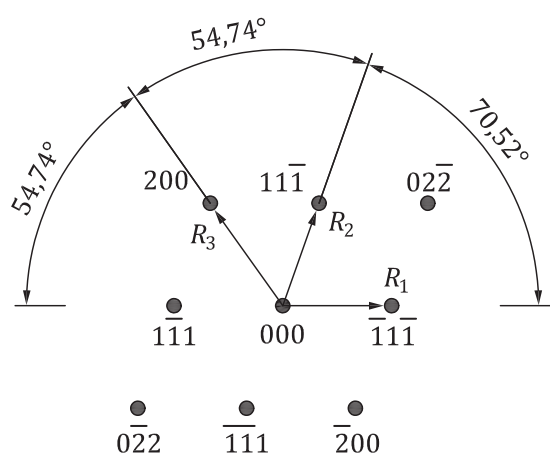
Spot diffraction patterns from a single crystal with FCC structure, for $(u^2+v^2+w^2) \leq 22$ are given in [Figures B.15 to B.28](#).



Key

$R_2/R_1 = 1,000$
 $R_3/R_1 = 1,414$

Figure B.15 — $[uvw] = [001]$ for FCC

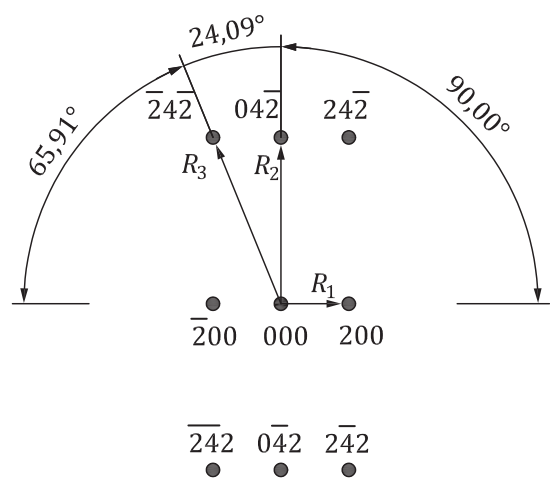


Key

$R_2/R_1 = 1,000$

$R_3/R_1 = 1,155$

Figure B.16 — $[uvw] = [011]$ for FCC

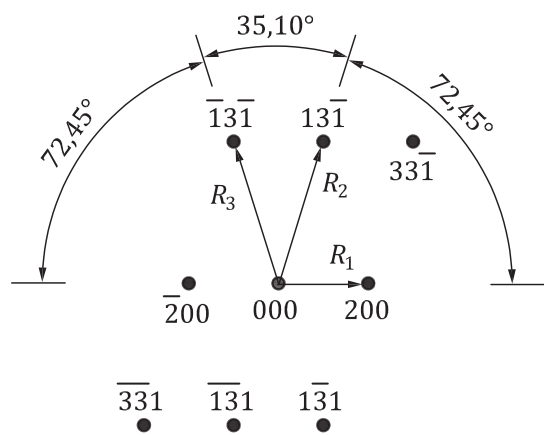


Key

$R_2/R_1 = 2,236$

$R_3/R_1 = 2,450$

Figure B.17 — $[uvw] = [012]$ for FCC

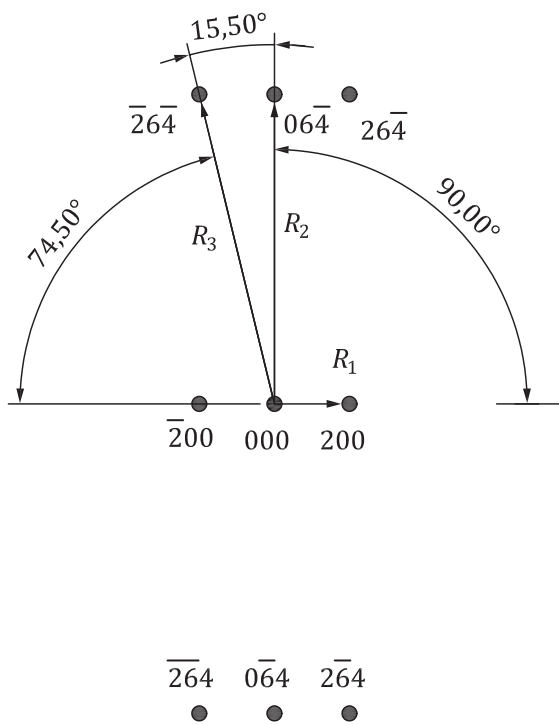


Key

$R_2/R_1 = 1,658$

$R_3/R_1 = 1,658$

Figure B.18 — $[uvw] = [013]$ for FCC

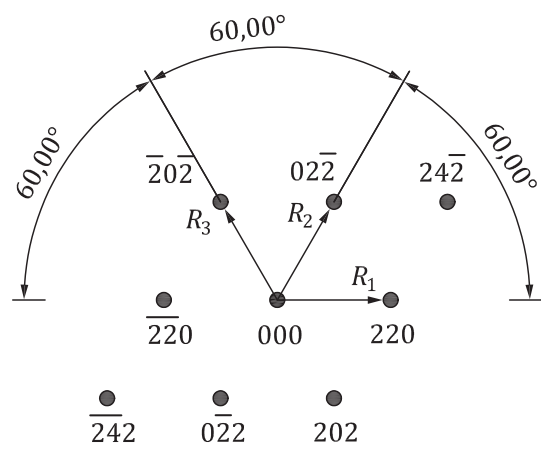


Key

$R_2/R_1 = 3,606$

$R_3/R_1 = 3,742$

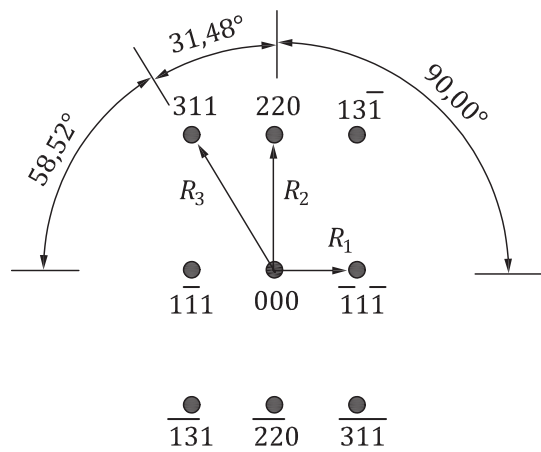
Figure B.19 — $[uvw] = [023]$ for FCC



Key

$R_2/R_1 = 1,000$
 $R_3/R_1 = 1,000$

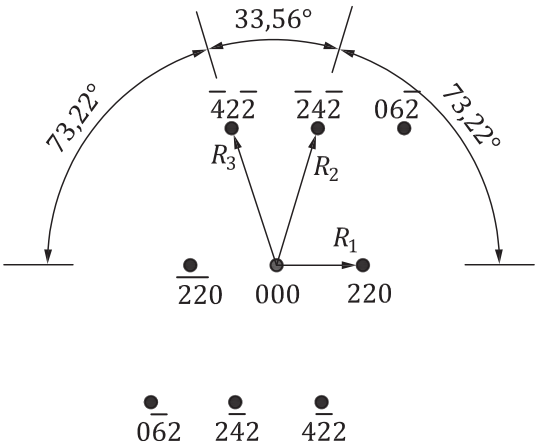
Figure B.20 — $[uvw] = [\bar{1}11]$ for FCC



Key

$R_2/R_1 = 1,633$
 $R_3/R_1 = 1,915$

Figure B.21 — $[uvw] = [\bar{1}12]$ for FCC

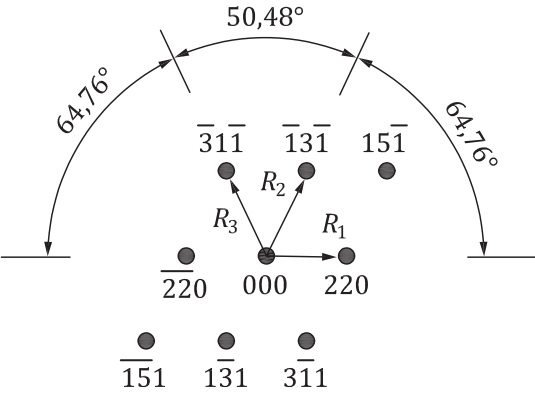


Key

$R_2/R_1 = 1,732$

$R_3/R_1 = 1,732$

Figure B.22 — $[uvw] = [\bar{1}13]$ for FCC

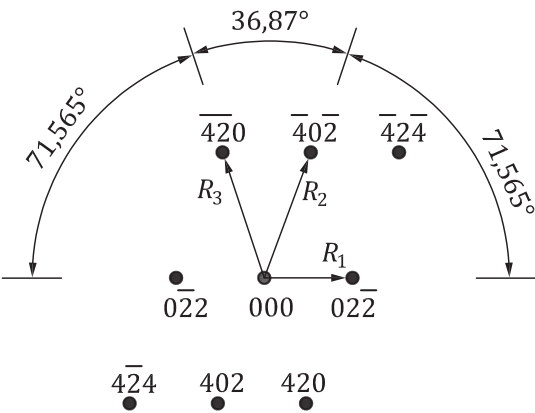


Key

$R_2/R_1 = 1,173$

$R_3/R_1 = 1,173$

Figure B.23 — $[uvw] = [\bar{1}14]$ for FCC

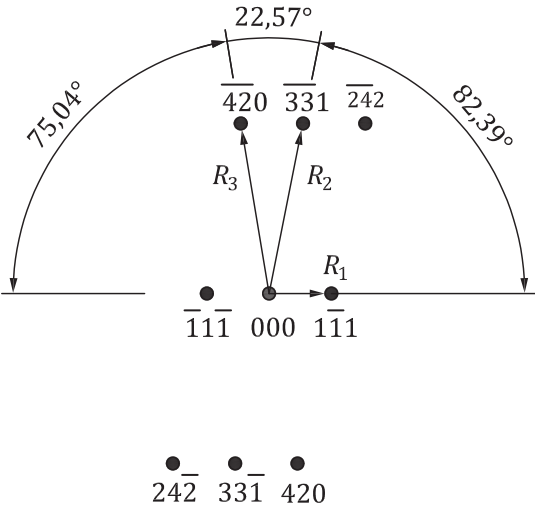


Key

$R_2/R_1 = 1,581$

$R_3/R_1 = 1,581$

Figure B.24 — $[uvw] = [\bar{1}22]$ for FCC

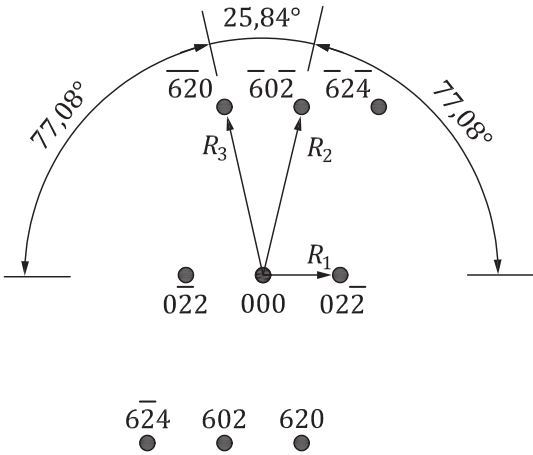


Key

$R_2/R_1 = 2,517$

$R_3/R_1 = 2,582$

Figure B.25 — $[uvw] = [\bar{1}23]$ for FCC

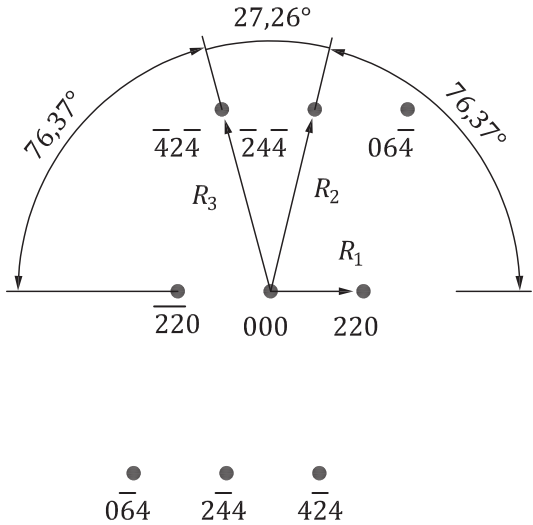


Key

$R_2/R_1 = 2,236$

$R_3/R_1 = 2,236$

Figure B.26 — $[uvw] = [\bar{1}33]$ for FCC

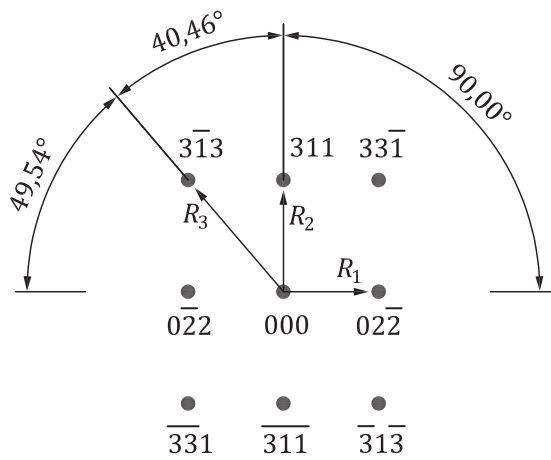


Key

$R_2/R_1 = 2,121$

$R_3/R_1 = 2,121$

Figure B.27 — $[uvw] = [\bar{2}23]$ for FCC



Key

$R_2/R_1 = 1,173$

$R_3/R_1 = 1,541$

Figure B.28 — $[uvw] = [\bar{2}33]$ for FCC

B.4 Spot diffraction patterns for hexagonal close-packed (HCP) crystals

B.4.1 General

Spot diffraction patterns from single crystal with HCP structure (for $c/a = \sqrt{8/3} \cong 1,633$) are given in [Figures B.29](#) to [B.40](#). Miller-Bravais notation is used for indexing the diffraction patterns of HCP crystals. Miller notation may also be used for the indexing.

NOTE The symbol, ✕, denotes the forbidden diffracted spots, which can occur due to the secondary diffraction.

B.4.2 Index conversion between Miller-Bravais notation and Miller notation

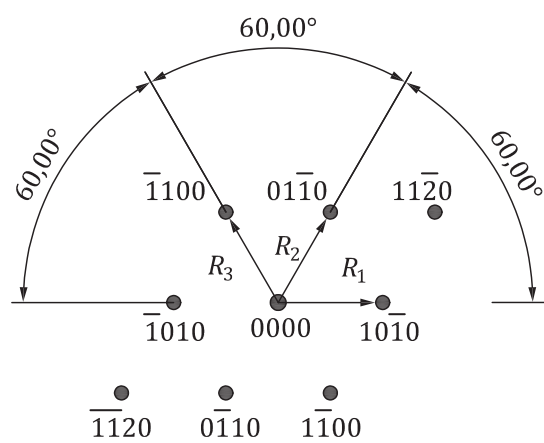
The index conversion between Miller-Bravais notation $[UVTW]$ and Miller notation $[uvw]$ for a zone axis may be carried out by using [Formulae \(B.1\)](#) and [\(B.2\)](#) respectively.

$$u = U - T, v = V - T, w = W \tag{B.1}$$

$$U = \frac{1}{3}(2u - v), V = \frac{1}{3}(2v - u), T = -\frac{1}{3}(u + v), W = w \tag{B.2}$$

The relationship between Miller-Bravais notation $(hkil)$ and Miller notation (hkl) of a plane is given by [Formula \(B.3\)](#).

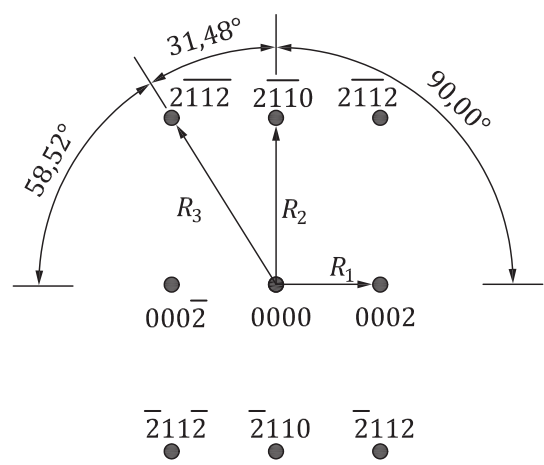
$$i = -(h + k) \tag{B.3}$$



Key

$R_2/R_1 = 1,000$
 $R_3/R_1 = 1,000$
 $[UVTW]=[0001]$

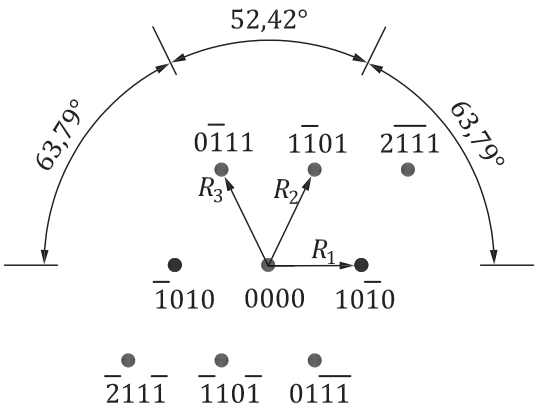
Figure B.29 — $[uvw] = [001]$ for HCP



Key

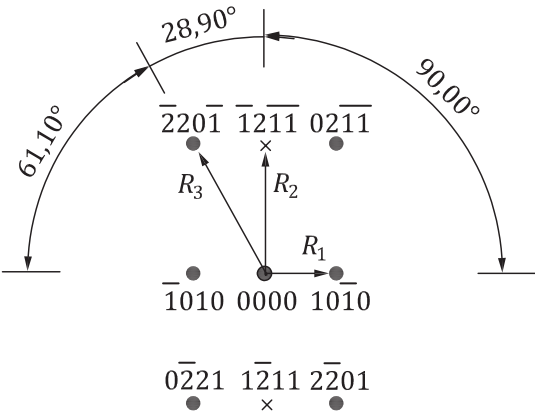
$R_2/R_1 = 1,633$
 $R_3/R_1 = 1,915$
 $[UVTW]=[01\bar{1}0]$

Figure B.30 — $[uvw] = [120]$ for HCP



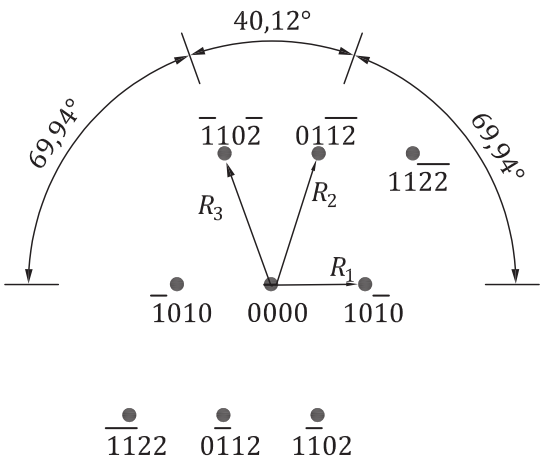
Key
 $R_2/R_1 = 1,132$
 $R_3/R_1 = 1,132$
 $[UVTW] = [\bar{1}2\bar{1}3]$

Figure B.31 — $[uvw] = [011]$ for HCP



Key
 $R_2/R_1 = 1,812$
 $R_3/R_1 = 2,069$
 $[UVTW] = [\bar{1}2\bar{1}6]$

Figure B.32 — $[uvw] = [012]$ for HCP



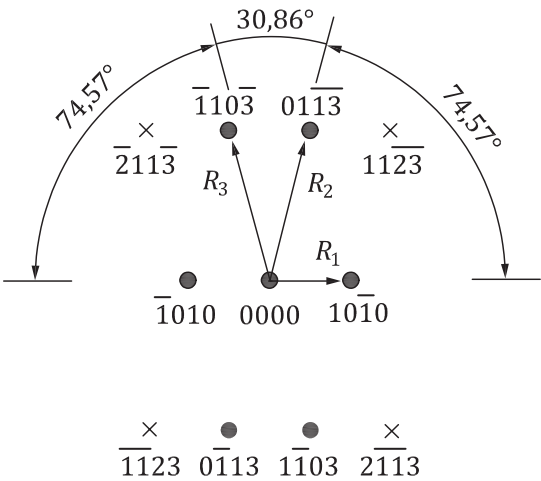
Key

$R_2/R_1 = 1,458$

$R_3/R_1 = 1,458$

$[UVTW] = [\bar{2}4\bar{2}3]$

Figure B.33 — $[uvw] = [021]$ for HCP



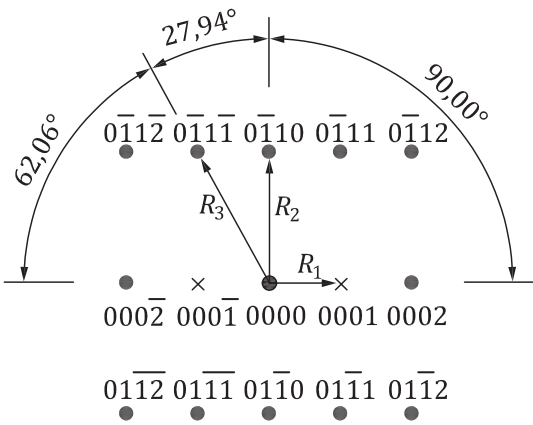
Key

$R_2/R_1 = 1,880$

$R_3/R_1 = 1,880$

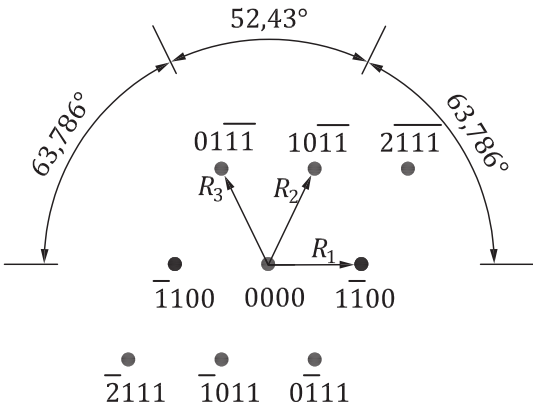
$[UVTW] = [\bar{1}2\bar{1}1]$

Figure B.34 — $[uvw] = [031]$ for HCP



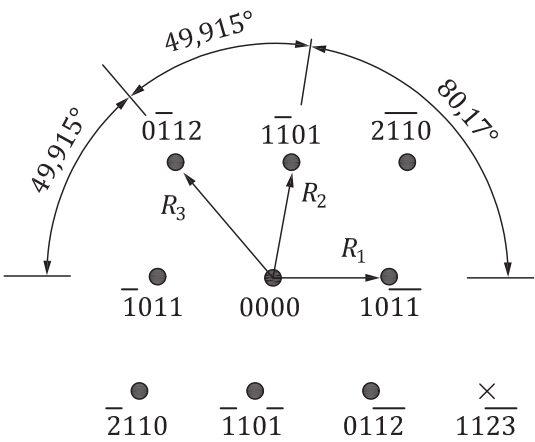
Key
 $R_2/R_1 = 1,887$
 $R_3/R_1 = 2,134$
 $[UVTW] = [2\bar{1}10]$

Figure B.35 — $[uvw] = [100]$ for HCP



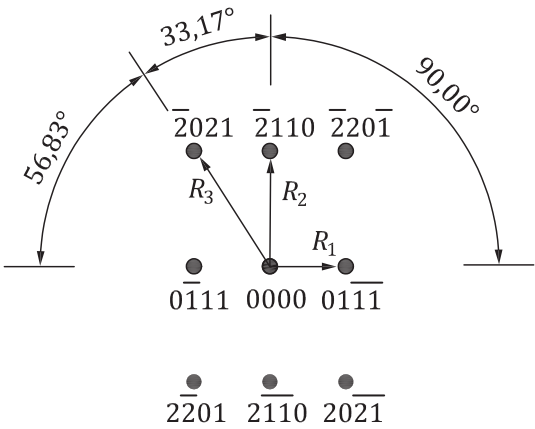
Key
 $R_2/R_1 = 1,132$
 $R_3/R_1 = 1,132$
 $[UVTW] = [11\bar{2}3]$

Figure B.36 — $[uvw] = [111]$ for HCP



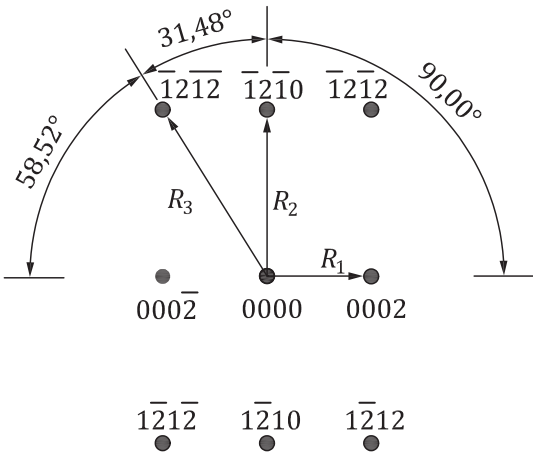
Key
 $R_2/R_1 = 1,000$
 $R_3/R_1 = 1,288$
 $[UVTW] = [01\bar{1}1]$

Figure B.37 — $[uvw] = [121]$ for HCP



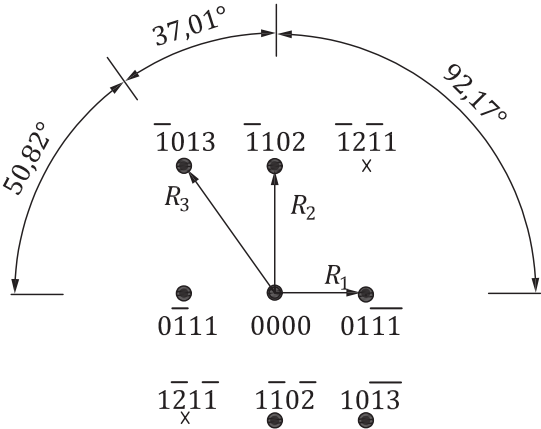
Key
 $R_2/R_1 = 1,530$
 $R_3/R_1 = 1,828$
 $[UVTW] = [01\bar{1}2]$

Figure B.38 — $[uvw] = [122]$ for HCP



Key
 $R_2/R_1 = 1,633$
 $R_3/R_1 = 1,915$
 $[UVTW] = [10\bar{1}0]$

Figure B.39 — $[uvw] = [210]$ for HCP



Key
 $R_2/R_1 = 1,288$
 $R_3/R_1 = 1,660$
 $[UVTW] = [5\bar{1}43]$

Figure B.40 — $[uvw] = [311]$ for HCP

Bibliography

- [1] ISO/IEC 17025, *General requirements for the competence of testing and calibration laboratories*
- [2] ASTM E 3-11, *Standard practice for preparation of metallographic specimens*
- [3] Liu D.L., Features of the ISO-25498: Method of Selected Area Electron Diffraction Analysis in Transmission Electron Microscopy, *Microsc. Microanal.* 19, S5, 207–209, 2013
- [4] Williams, D.B. and Carter, C.B. *Transmission Electron Microscopy: A Textbook for Materials Science*, Plenum Press, New York 2009
- [5] Edington, J.W. *Practical Electron Microscopy in Materials Science, Vol. II, Electron Diffraction in The Electron Microscope*, Macmillan & Co Ltd, London, 1975
- [6] Guo, K.X., Ye, H.Q., Wu, Y.K., *Application of electron diffraction patterns in crystallography*, Science Press, China, 1983(in Chinese)
- [7] Andrews, K.W., Dyson, D.J., Keown, S.R. *Interpretation of electron diffraction patterns*, Second Edition, 1971. (Publisher Hilger, London, ISBN-0-85274-170-7)
- [8] Reimer, L., *Transmission Electron Microscopy*, 4th Edition, Springer, 2004
- [9] Fultz, B, Howe, J., *Transmission Electron Microscopy and Diffractometry of Materials*, 3rd Edition Springer Berlin Heidelberg New York 2008
- [10] Goodhew, P.J. *Specimen preparation for transmission electron microscopy of materials*, Oxford University Press, Royal Microscopical Society, 1984
- [11] Ayache, J., Beaunier, L., Boumendil, J., Ehret, G., Laub, D., *Sample Preparation Handbook for Transmission Electron Microscopy*, Springer New York Dordrecht Heidelberg London, 2010
- [12] The Powder Diffraction File 1997–2007, JCPDS, International Centre for Diffraction Data (ICDD)
- [13] Jiang, L, Georgieva, D., Zandbergen, H.W. and Abrahams, J.P. (2009) Unit-cell determination from randomly oriented electron-diffraction patterns. *Acta Cryst. D*, 625-632
- [14] <https://www.iucr.org/resources/other-directories/software/ediff>
- [15] ISO/IEC Guide 98-3:2008, *Uncertainty of measurement — Part 3: Guide to the expression of uncertainty in measurement (GUM:1995)*
- [16] Swanson, Tatge, Natl. Bur. Stand. (US), Circ. 539,1,11 (1953)



ICS 71.040.50

Price based on 42 pages